Case study of PP and PS seismic response from fractured tight gas reservoirs

Jianming Tang, SinoPec Southwest Limited, Shaonan Zhang, Chengdu University of Technology, Xiang-Yang Li, Edinburgh Anisotropy Project, British Geological Survey*

Summary

In this paper, we present an example of using PP and PS seismic data recorded by digital MEMS (micro-eletro-mechanical-system) sensors to evaluate a fractured tight gas reservoir from the Xinchang gas field in Sichuan China. We analyze the variations in converted shear-wave splitting, Vp/Vs ratio and PP and PS impedance, as well as other attributes based on absorption and velocity dispersion. The reservoir formation is tight sandstones, buried at the depth about 5000m, and the converted shear-wave data reveal significant shear-wave splitting over the reservoir formation. We utilize a rotation technique to separate the fast and slow shear-waves, and a small-window correlation method to build time-delay spectra that allows the generation of a time-delay section. At the reservoir formation, the interval shear-wave anisotropy is about 12%, correlating with the known gas reservoirs. Furthermore, the splitting anomalies are consistent with the characteristics showing in other attributes such as Vp/Vs ratio and P- and S-wave acoustic and elastic impedance. The P-wave shows consistent low impedance over the reservoir formation, whilst the S-wave impedance shows no obvious variation. The calculated gas indicator based on absorption and velocity dispersion yields a high correlation with the gas bearing formations.

Introduction

Recently, the use of digital MEMS (micro-electro-mechanical system) sensors has substantially improved the quality of land converted-wave data (e.g. Calvert et al., 2005). As a result, here we present an example of using MEMS-based converted-wave technology for evaluating fractured tight-sandstone gas reservoirs from the Sichuan gasfields in Southwest China. The Sichuan province is one of largest gas province in China, and gas production in Sichuan is mainly from deep buried tight sandstone and carbonates at depths from 4000m to 6000m (Figure 1a). Fracture characterization is critical for ensuring economic gas production from these tight formations of otherwise low permeability (Li, 1997). The use of P-wave techniques for characterizing these fractures has not been very successful in this area due to the depth limitations. Success of past multicomponent seismic experiments is also limited due to data quality issues. The advent of MEMS sensors has renewed the interest to use PP and PS multicomponent seismic data in this area. As a result, new multicomponent experiments were carried out subsequently. Three 2D3C test lines were acquired during a 3D3C multicomponent experiment conducted in 2005, and the results of the test lines are presented in this paper.

The geological setup

The study area is located in the Sichuan Province in Southwest China. The ancient apophysis and inclines formed in the Indosinian and Yanshanian periods were good traps for gas accumulation. Early reservoirs were closed in the deep tight sandstones. Structure and fault (fracture) caused by uplift and pressure deformation in the Himalayan Period made some early gas deposits migrate to the upper Jurassic formation and accumulate along faults and fractures in the formation. Meanwhile the early gas reservoirs in the deeper formations were activated and re-grouped into places where porosity and permeability were relatively higher and fracture growth was intensive, finally forming many new and rich reservoirs such as the Xinchang field near Chengdu, the provincial capital of Sichuan. This is the basic geological setup for the formation of highly productive gas reservoirs in this area.

Petrophysical analysis of the core samples shows that the average matrix porosity is less than 3%, average matrix permeability is less than $0.1\times10^{-3}\mu m^2$ for most of the core samples taken from the field. Thus, these reservoirs are classified as deep buried tight sandstone reservoirs with low porosity and permeability.

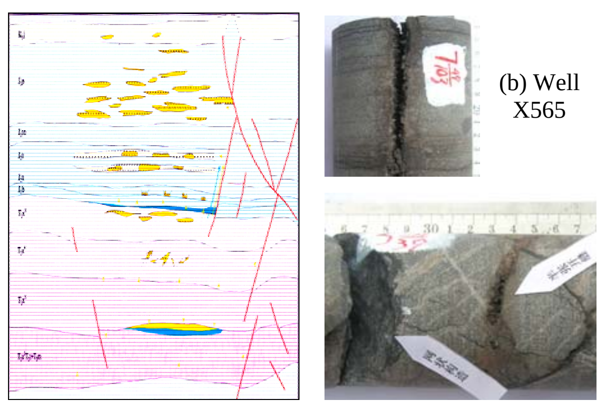

(a) Reservoir pattern (c) Well X853

Figure 1: (a) A typical geological section showing the gas reservoir patterns, and (b) and (c) core samples from the study area.

The presence of near vertical fractures, giving rise to horizontal transverse isotropy (HTI), is critical to ensure economic production in the Xinchang Gas Field. As shown in Figures 1b and 1c, core samples reveal intensive fracturing in the target formation. Analysis of the distribution of low- and high-angle fractures with productivities from four boreholes in the Xinchang field confirms the importance of the presence of near vertical high-angle fractures.

Data acquisition and characteristics

The experiment consists of three 2D lines with about 45km of full-fold coverage, as shown in Figure 2a, where the red box shows the 3D coverage. Line 1(L1) and Line 2(L2) are orthogonal to each other, and Line 3(L3) is at 45º angle to L1 and L2. The three lines form an intersection point at well X851, which is the most productive well in the region. To help static correction for processing converted-waves, refraction surveys (blue points, Figure 2b) and multicomponent uphole (red points, Figure 2b) were conducted during acquisition.

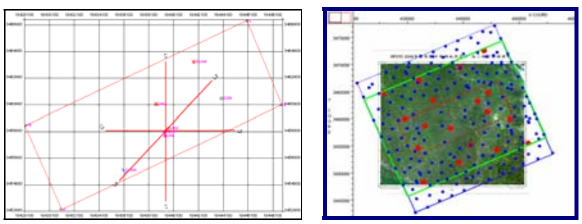

(a) Layout of the test lines (b) Near surface surveys

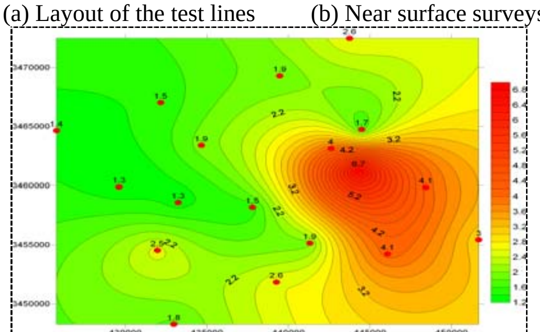

(c) The near surface Vp/Vs model

Figure 2: The acquisition programme: (a) Acquisition layout of the test lines, and the red box indicates the 3D coverage, (b) locations of micro-refraction surveys marked by the blue points and multicomponent uphole marked by the red points, and (c) the near surface Vp/Vs model derived from the surveys in (b).

All the lines were acquired with a split spread with a maximum offset of 8640m, nominal receiver interval of 40m, and shot interval of 120m. The use of digital MEMS sensors has lead to the acquisition of very high quality shear-wave data (Figure 3), although some ground roll can be observed. Dominant frequency is about 40hz for P-wave and about 20hz for converted-wave. There is a significant amount of energy present in the crossline (Y) component, indicating the presence of shear-wave splitting.

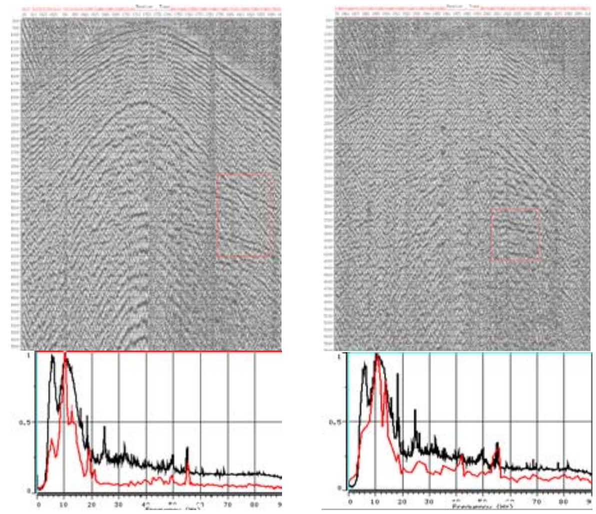

(a) Inline -x (b) Crossline –y

Figure 3. Sample shot records from Line 3 and their corresponding frequency spectra: (a) inline and (b) crossline horizontal components. The black curves in the spectra are calculated from the whole trace, and the red curves are calculated from the selected windows indicated by the red rectangles in the shot records.

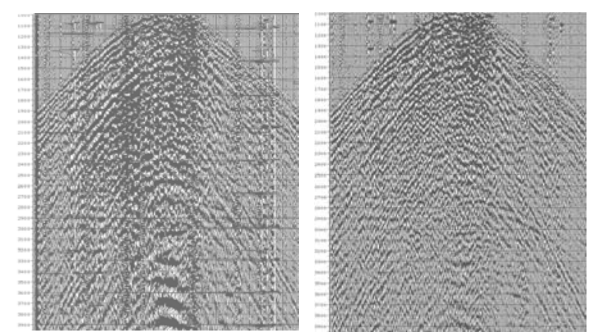

Original After noise reduction

Figure 4. Comparison of the results of noise reduction, and the input data is a shot record of the inline X-component from Line 3. (a) Original data and (b) results after applying a model-based technique (Qian and Zhao, 2003).

Data processing

For this data, the target formation is very deep, and the non-hyperbolic moveout effects are relatively weak, and noise and statics are the main issues for processing the converted-wave data in this case. For noise reduction, we test different techniques for reducing the ground roll, including a deterministic model-based technique (Qian and Zhao, 2003), and the conventional F-K filtering technique. The model-based technique is very effective in removing the ground roll and other noise (Figure 4).

Our strategy to solve the static problem is through data acquisition. For this, a micro-refraction survey with coverage of 2kmx2km, totally 200 points was conducted to investigate the P-wave near surface velocity model, as marked by the blue points in Figure 2b. In addition eighteen multicomponent upholes were recorded for determining the near-surface Vp/Vs model, as marked by the red points in Figure 2b. The near surface S-wave velocity model can then be calculated from these measurements. This gave us a very good control of the near surface velocity model, and the values of Vp/Vs vary from 1.5 to 6.7 (Figure 2c). Although this increased the cost of the experiment, it did provide a good solution to the notorious shear-wave static problem.

Due to the improved data quality and near-surface data availability, the processing is relatively straightforward. For the three test lines, the P-wave shows little difference in amplitude and waveform, indicating no observable azimuthal variation; there is also no-observable mistie at the well location. However, there are clear misties in the horizontal components at the well location among the three lines. L3 is of the highest quality; the events are strong and continuous. At the target formation, the events on the X-component are faster than those on the Y-component, and the time delay is about 20ms (Figure 5).

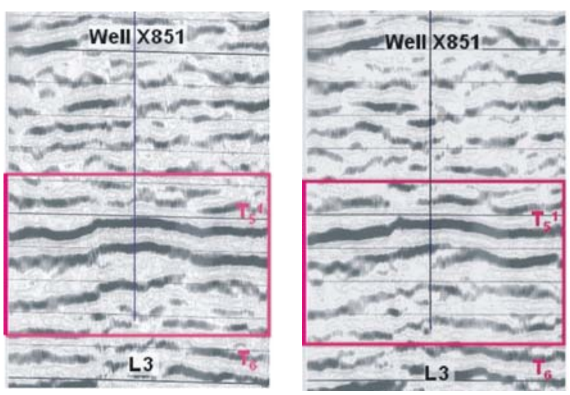

(a) Inline X (b) Crossline Y

Figure 5. Final stacked sections of the horizontal (a) X- and (b) Y-components of Line L3. The red boxes highlight the target.

Analysis of shear-wave splitting

We apply a rotation scanning procedure to the X- and Y-component data, which maximizes the separation of the fast and slow shear-waves (Yuan, 2001). Once the split shear-waves are separated, a small-window correlation method can be used to construct a time-delay spectrum (Figure 6a) between the fast and slow shear waves, from which a time-delay section can be obtained for interpretation purposes. Figure 6b shows a time-delay gradient section (Line L3) intersecting well X851, superimposed by the stacked seismic section. As shown in Figure 6b, areas of high gas accumulation show a significant amount of splitting (well X851). The splitting anomalies seem to be good indicators of gas accumulation, and can be used to delineate the fractured reservoirs.

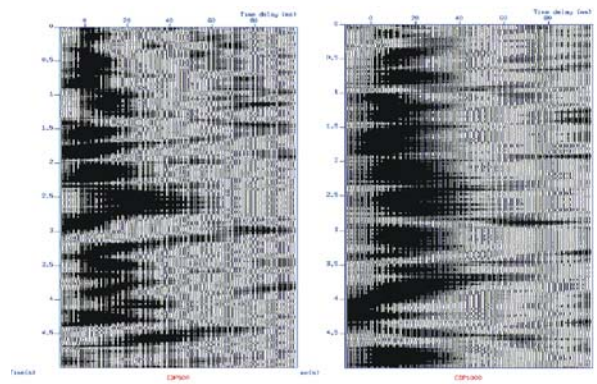

(a) Time-delay spectra

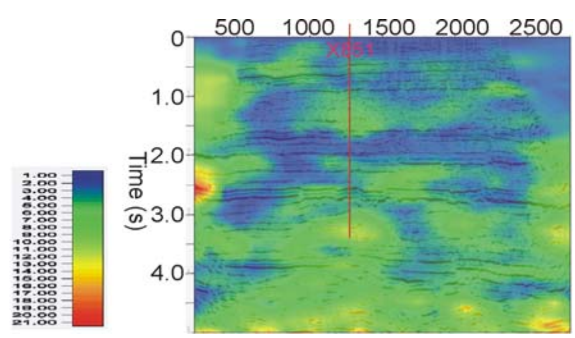

(b) Time-delay gradient section

Figure 6. Shear-wave splitting analysis: (a) Calculated time-delay spectra of the split shear-waves for Line L3, and (b) interpretation results of the time-delay gradient section superimposed by the corresponding seismic section. X851 is the most productive gas well in the study area, which is drilled into a zone with more than 12 % shear-wave anisotropy. The color bar on the left indicates percentage shear-wave splitting.

Analysis of P and S-wave impedance

These include acoustic impedance sections inverted from the Z-component, shear impedance sections inverted from the horizontal X-component, elastic impedance at incidence angle of 30^0 and the derived Vp/Vs ratio sections from the inverted acoustic and shear impedance (Figure 7). There are two main pay beds in the study area, pay bed $TX_2 4$ as encountered by well X851 at 2.4 seconds, and $TX_2 6$ as encountered by well X853 at 2.5 seconds. We can see clear low impedance (blue color) in the Vp/Vs ratio sections (Figure 7), which agrees with the sonic logs in Figure 8. There are clear anomalies associated with the gas sands, as indicated by the yellow colors in Figure 8. These observations confirm the results of impedance inversion. A combined attribute based on absorption and velocity dispersion of the P- and S-waves may also be derived from the data, as shown in Figure 9, where a clear and better correlation between the anomalies and the pay beds can be observed.

Discussion and conclusions

We have shown a case study of using multicomponent data for delineating fractured gas reservoirs in tight sandstone formations. The target formation is buried at depth of more than 5000m, and consequently the non-hyperbolic moveout effects are not very significant and simple straightforward processing can be applied to the converted-wave data. Conducting of detailed refraction surveys and recording of multicomponent uphole time are very beneficial for providing an accurate solution to the shear-wave static problem, although it increases the cost of acquisition.

In terms of gas reservoir response, the PP- and PS-attributes show consistent anomalies that diagnose the presence of fractured gas sands. First, significant shear-wave splitting is observed at the target formation, and area of high gas accumulation can be correlated with the amount of shear-wave splitting. Secondly, low acoustic and elastic impedance inverted from the P-wave data can be observed at the zone of interests, and a consistent low Vp/Vs ratio can also be observed at the fractured gas sands. Thirdly, a combined attributed measuring the absorption and velocity dispersion also show consistent anomalies associated with the gas sands. This confirms the benefit of multicomponent seismic data.

Acknowledgements

We thank SinoPec Southwest Ltd. for permission to show the data. We thank Mr. Zhang Yonggang for coordinating this project. This work is supported by the SinoPec international collaboration programme and SinoPec Southwest Ltd. through the Edinburgh Anisotropy Project (EAP) of the British Geological Survey (BGS), and is published with the approval of all project partners and the Executive Director of BGS (NERC).

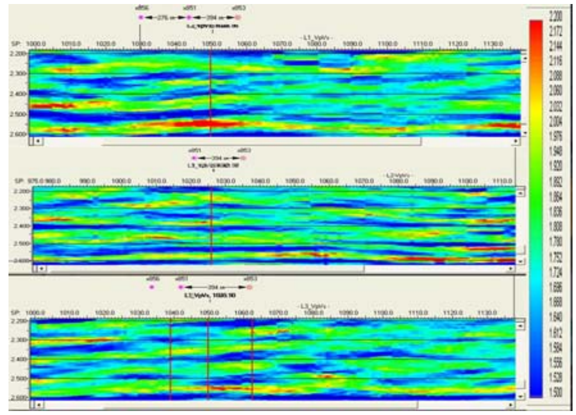

Figure 7. Calculated Vp/Vs ratio sections from the inverted P- and S-wave impedance at the zones of interest for lines L1 (top), L2 (middle) and L3 (bottom).

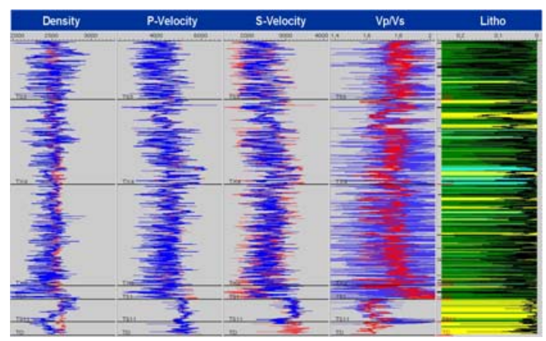

Figure 8: Sonic logs and lithology from borehole X851. Yellow color at the lithology log at the far right stands for gas sand, green for shale, and light blue for calcite.

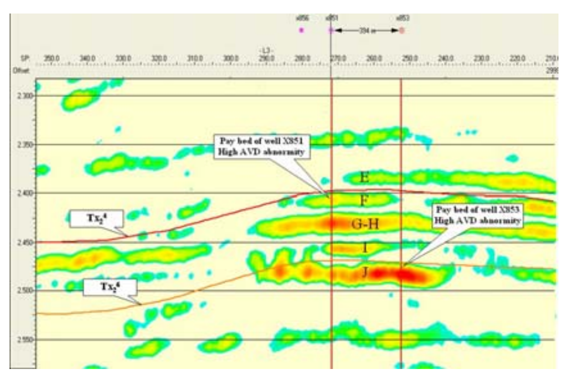

Figure 9: Absorption and velocity dispersion calculated from the P- and S-wave data for Line L3.

References

Calvert, A.S., Novak, J.M., Maher, J., Burch, D.N., Bird, D., Larson, R., 2005, A tale of two surveys: experiences processing two similar but different land 3D-3C MEMS surveys: 75th SEG meeting, Houston, USA, Expanded Abstracts, 975-978.

Li, X.-Y., 1997, Fractural reservior delineating using multicomponent seismic data: Geophysical Prospecting, **54**, 39-64.

Qian, Z. and Zhao, B., 2003, A regular noise elimination method for prestack 3D seismic data: 73rd SEG Meeting, Dallas, Expanded Abstracts, 2040-2043.

Yuan, J. 2001, Analysis of four-component sea-floor seismic data for seismic anisotropy: PhD Thesis, University of Edinburgh.